SCIENCE

NUMERICAL SIMULATION OF STEADY VISCOUS FLOW PAST TWO ROTATING CIRCULAR CYLINDERS

Surattana Sungnul* **and Nikolay Moshkin**

Received: Mar 31, 2006; Revised: May 24, 2006; Accepted: May 30, 2006

Abstract

The present work deals with the laminar flow of a uniform stream past two circular rotating cylinders. The principal feature of interest is that the rotation of the cylinders leads to a zero drag force on the cylinders. This case corresponds to self-propelled motion of cylinders as a coupled body. The case of equal contra-rotating cylinders is considered, with the stream normal to the plane containing the axes of the cylinders. The components of the resultant force on the cylinders are determined by the numerical solution of the incompressible two-dimensional Navier-Stokes equations in the cylindrical bipolar coordinate system. Both self-motion and towed regimes of fluid flow are considered.

Keywords: Rotating circular cylinders, viscous incompressible fluids, self-propelled

Introduction

The problem of flow past two rotating circular cylinders in a viscous fluid has long attracted mathematicians and engineers. This flow shows some analytical peculiarities regarding the implementation of near-field and far-field boundary conditions. It might be for this reason that the flow has attracted much interest from theoretical fluid dynamicists. It is impossible, in general, to obtain solutions of Stokes' equations of slow viscous steady flow in which the fluid velocity vanishes at infinity (Jeffery, 1922). If the cylinders are outside one another, Jeffery found that it is impossible, in general, to make the fluid velocity vanish at infinity. He illustrated this by a detailed treatment of the case of equal cylinders, rotating with equal speeds in an opposite sense. This is the Jeffery paradox. To resolve this paradox, Smith (1991) obtained an asymptotic solution of the Stokes equations for the stream function which is valid at large distances from the cylinders. This asymptotic expansion involves many unknown coefficients of the Fourier series and there was no obvious way as to how these may be obtained. Elliott *et al.* (1995) established the boundary element method by using the asymptotic expansions given by Smith and showed numerically that the combined bodies have no overall force or torque acting upon them. Watson (1995) pointed out that the pressure field given by Smith's asymptotic form is not single-valued and proposed that an additional term to Jeffery's Fourier series is necessary. However, he did not derive the force, since the outer flow which is

School of Mathematics, Institute of Science, Suranaree University of Technology, Nakhon Ratchasima 30000, Thailand. E-mail: suratana@math.sut.ac.th

* *Corresponding author*

governed by the Navier-Stokes equations was not obtained.

The problem of flow past rotating cylinders was considered by Sennitskii (1973). The problem was studied using a boundary layer approach for the case of a large distance between the center of cylinders. In the work of Sennitskii (1975a) the first terms of an asymptotic expansion by inverse degree of the Reynolds number were obtained. Using symptotic expansion by degree of the small parameter which is the ratio of the cylinder radius to the distance between the axes of cylinders, the problem of stationary flow past rotating cylinders was solved approximately by Sennitskii (1975b). It was ascertained that, in the approximation considered, the pair of rotating cylinders is a self-propelled body. In connection with the problem of decreasing the energy required for a body to move in a liquid, the motion of a pair of rotating cylinders in a liquid was also investigated experimentally (Sennitskii, 1980, 1981).

In pure motion by self-propulsion the total net force and torque, external to the system body-fluid, acting on the body are zero. The forward force (thrust) that makes the body move is generated by the body itself and the motion is due to the interaction of the body's external surface and the fluid in which it is immersed. The hydrodynamic mechanism of self-propulsion is different for macroscopic and microscopic bodies. Large objects which propel themselves make use of inertia in the surrounding fluid. Their thrust can be produced by muscular action and change of shape, as in animal locomotion, or can be provided by mechanical propulsion systems, as in an airplane, rocket or submarine (Milne-Thomson, 1952).

Though the problem of a self-propelled body has a natural origin and though it is of practical importance, the number of works concerning it is very limited. Before explaining the objectives and results of this paper, let us briefly refer to the literature on the mathematical analysis and numerical simulations of motion by self-propulsion of a rigid body in an infinite Navier-Stokes fluid. In Finn (1965) and Pukhnachev (1989, 1990) the asymptotic properties of steady flow past a self-propelled body moving with purely translational velocity are investigated. The existence of such solutions was first established for very particular shapes, like balls and cylinders in Sennitskii (1978, 1984, 1990) and for a symmetric body around an axis in Galdi (1997). Considering the general form of a rigid body motion, with the rotation of the body taken into account, Galdi (1999) proved the existence of steady self-propelled solutions for a body with arbitrary geometry, with a detailed study of the cases of zero and nonzero Reynolds numbers. In Silvestre (2002a, 2002b) the existence of a weak solution to the general unsteady nonlinear problem and the attainability of steady purely translational self-propelled motion for a symmetric body was proved. In Sennitskii (1978, 1984, 1990), by methods consistent with asymptotic decomposition for a low Reynolds number, the flow past a circular cylinder with a moving boundary and of flow past a ball with a liquid-permeable boundary was investigated. The asymptotic formulas for the velocity at great distance from the body were obtained. More rapid decay of velocity perturbation at a larger distance from a self-moving body than a towed one were noted. Lugovtsov (1971) examples of flat potential viscous flow past a self-moving "body" are studied. Its boundary consists of two symmetrical coupled components. On each the normal velocity components are equal to zero and the tangential components are constant.

A numerical solution to the problem of momentumless flow past an extended ellipsoid of rotation was obtained by Izteleulov (1985). A propelling model is a self-consistent distribution of volume force located in a small region behind the body. Simulation of the problem of conductive incompressible viscous flow past the body in an electromagnetic field was considered in Shatrov and Yakovlev (1985) and Khonichev and Yakovlev (1978). In papers of Moshkin *et al.* (1989) and Moshkin (1991) two particular cases of self-motion were considered by numerical solution of the Navier-Stokes equations. In one of them there is a surface behind (downstream) the ball. The liquid flows through this surface and gets there by an additional momentum.

In the other case the ball surface is permeable. On one of its parts, between two cones with the divergence semi-angles Θ_1 and Θ_2 and a mutual axis $\Theta = \pi$, the liquid is sucked in, and on the other part, 'cut' by a cone $\Theta_3 \le \Theta \le \pi$, the same quantity of the liquid is returned to the flow. In the paper of Nakanishi and Kida (1999) the vortex method was applied to a low Reynolds number unsteady flow generated by two circular cylinders of equal radii set rotating abruptly with equal angular velocities in a flow initially at rest. Elliot *et al.* (1995) developed the boundary element method by using the asymptotic expansions and showed numerically that the combined bodies (two cylinders) have no overall force or torque acting upon them.

According authors knowledge there are no detail study of problem of flow past two rotating circular cylinders for moderate Reynolds numbers. Particularly, there are no comparisons between self-propelled and towed regime of motion, there are no consistent set of data for the drag and lift forces for moderate Reynolds numbers and moderate rate of cylinder's rotation

In this paper, we shall be interested in the self-propulsion of a rigid body. The shape of the body is constant during the motion, and the thrust is produced because the body boundary moves. The motion of the body is therefore completely determined by its geometry and by the distribution of the velocity on its boundary. In fact, the combined body which consists of two rotating circular cylinders is an example where self-propelled motion is due to a non-zero velocity of the boundary. We shall study not only self-motion of rotating cylinders but also flow past towed cylinders. Different rotation of cylinders can be considered as a propulsion device for controlling the motion of the body. The plan of the paper is the following. In Section 2 we introduce the mathematical formulation for the self-propelled motion problem in general and for the particular case of two rotating cylinders. In Section 3 we introduce the numerical scheme used for the approximate solution of the Navier-Stokes equation with boundary conditions. In Section 4 we present the data for validation of our numerical algorithm by comparison with available solutions and experimental data. Section 5 is dedicated to the main results of numerical simulation and is concerned with the self-propelled motion as well as fluid flow past two towed rotating circular cylinders in a uniform stream.

Mathematical Formulation

General Case of Arbitrary Rigid Body

To better explain our results, let us first give a mathematical formulation of the problem in the general case. We represent a rigid body by a compact set $\mathcal{B}$ that is moving in a viscous fluid $\mathcal{L}$ which occupies the region $\mathcal{D} = \mathcal{R}^3 / \mathcal{B}$ exterior to the body. The motion of $\{\mathcal{B}, \mathcal{L}\}$ is described by the following coupled system of equations and boundary conditions

$$\rho \frac{dv}{dt} = \mathrm{div}(T(v,p)), \text{ in } \mathcal{D} \times (0,\ T) \tag{1}$$

$$\mathrm{div}\ v = 0, \text{ in } \mathcal{D} \times (0,\ T) \tag{2}$$

$$v = v_*, \text{ at } \sum \times (0,\ T) \tag{3}$$

$$\lim_{x \to \infty} v(x,t) = 0, \text{ for } t \in (0,\ T), \tag{4}$$

$$m \frac{d\varsigma}{dt} = -\int_\Sigma T(v,p) \cdot n\, d\sigma, \text{ in } (0,\ T), \tag{5}$$

$$I \frac{d\omega}{dt} = -\int_\Sigma [x \times T(v,p)] \cdot n\, d\sigma, \text{ in } (0,\ T), \tag{6}$$

$$v(x,0) = v_0(x),\ x \in \mathcal{D} \tag{7}$$

$$\varsigma(0) = \varsigma_0,\ \omega(0) = \omega_0. \tag{8}$$

The quantities $v = v(x,t)$ and $p = p(x,t)$ represent the velocity and pressure associated with each particle of $\mathcal{L}$, $T(v,p)$ is the stress tensor, defined by

$$T_{ij}(v,p) = \mu \left\{ \frac{\partial v_i}{\partial x_j} + \frac{\partial v_j}{\partial x_i} \right\} - p\delta_{ij},$$

$$i, j = 1, 2, 3, \tag{9}$$

where μ is the coefficient of dynamic viscosity. The field $V(x,t) = \varsigma(t) + \omega(t) \times x$ represents the velocity of $\mathcal{B}$, $\varsigma(t)$ and $\omega(t)$ are velocity of center mass and vector of angular velocity of the body, respectively. In Eqns. (5) and (6) the positive constant m is the mass of $\mathcal{B}$ and I is its inertia tensor. Recall that

$$I_{ij} = \int_B \rho_B(x)(|x|^2 \delta_{ij} - x_i x_j)dx,$$

and I is a symmetric and positive definite (Danielson 1997). Here ρ_B is the mass density of the body $\mathcal{B}$. The distribution of velocity v_* on $\sum$ represents the thrust, responsible for the motion of the body. The two Eqns. (5) and (6) are consequences of Newton's laws of conservation of linear and angular momentum, respectively, for the body $\mathcal{B}$. Let us consider three possible cases.

a) If $\{\mathcal{B}, \mathcal{L}\}$ performs a steady motion then the left hand side of Eqns. (5), (6) are equal to zero. This is the case of self-propelled motion. One of the basic equations for this type of problem is the following one: in which way can we choose the field v_* in order that $\mathcal{B}$ moves with a (constant) rigid motion velocity $V = -\xi - \omega \times x$, where $\varsigma \neq 0$. Eqns. (5) and (6) with zero left hand side express the fact that the total external force and torque on $\mathcal{B}$ are identically zero, that $\mathcal{B}$ is a self-propelled body. In this case suitable distributions of velocity field v_* at $\sum$ are additional unknown quantities.

b) In the case of a towed body, the motion of $\mathcal{B}$ is due to external forces. The field $V(x,t) = \varsigma(t) + \omega(t) \times x$ is a known function of (x,t) and the velocity v_* on $\sum$ is also a given function. In this case we use integrals in the right hand side of Eqns. (5) and (6) to find the external drag force and torque on $\mathcal{B}$. In the simplest case, where $V(x,t) = \varsigma - const$ and $v_* = 0$ on $\sum$ the problem is fluid flow past the towed body. The direction of stream flow coincides with the direction of the vector V.

c) In the more general case Eqns. (1) - (9) represent the problem of rigid body motion in a viscous incompressible fluid due to the distribution velocity v_* on the boundary that furnishes the "thrust".

Representation of the Navier-Stokes Equations in Cylindrical Bipolar Coordinate System

It is natural to study the fluid flow in a boundary fitted curvilinear coordinate system. In order to study fluid flow past two circular cylinders, the reasonable coordinate system is the cylindrical bipolar coordinate system. The cylindrical bipolar coordinate system can be defined by the following equations

$$x = \frac{a \sinh \eta}{\cosh \eta - \cos \xi},$$

$$y = \frac{a \sin \xi}{\cosh \eta - \cos \xi}, \; z = z, \qquad (10)$$

where $\xi \in [0, 2\pi), \eta \in (-\infty, \infty), z \in (-\infty, \infty), a$ is a characteristic length in the cylindrical bipolar coordinate system which is positive. The following identities show that curves of constant ξ and η are circles in xy - space

$$x^2 + (y - a \cot \xi)^2 = a^2 \csc^2 \xi,$$

$$(x - a \coth \eta)^2 + y^2 = a^2 \operatorname{csch}^2 \eta. \qquad (11)$$

The coordinate surface $\eta = const$ corresponds to a family of nonintersecting cylinders whose centers lie along the $x-$ axis. The value $\eta = 0$ is a cylinder of infinite radius and is equivalent to the entire plane $x = 0$ Figure 1 shows two cylinders that are chosen to be $\eta = \eta_1$ (with $\eta_1 > 0$) and $\eta = \eta_2$ (with $\eta_2 < 0$). The cylinders' radii r_1 and r_2 and the distances of their centers from the origin d_1 and d_2 are given by

$$r_i = a \operatorname{csch} |\eta_i|, \; d_i = a \coth |\eta_i|, \; i = 1, 2. \qquad (12)$$

The center to center distance between the cylinders equals $d = d_1 + d_2$. If r_1, r_2 and d are given, one can find a, η_1 and η_2 from relations (10) - (12) as follows:

$$\eta_{1,2} = \ln\left[\left(\frac{d^2 + r_1^2 - r_2^2}{2dr_1}\right) \pm \sqrt{\left(\frac{d^2 + r_1^2 - r_2^2}{2dr_1}\right)^2 - 1}\right],$$

$$a = \sqrt{\frac{d^4 - 2d^2(r_1^2 + r_2^2) + (r_1^2 - r_2^2)^2}{4d^2}} \qquad (13)$$

The Navier-Stokes equations in the cylindrical bipolar coordinate system $(\xi, \eta\, z)$ are

$$\frac{\partial v_\xi}{\partial t} + \frac{1}{h}\left(v_\xi \frac{\partial v_\xi}{\partial \xi} + v_\eta \frac{\partial v_\xi}{\partial \eta}\right) + v_z \frac{\partial v_\xi}{\partial z}$$
$$-\frac{1}{a}\left(\sinh\eta (v_\xi v_\eta) - \sin\xi (v_\eta)^2\right) = -\frac{1}{h}\frac{1}{\rho}\frac{\partial p}{\partial \xi}$$
$$+\nu\frac{\partial^2 v_\xi}{\partial z^2} + \frac{\nu}{h}\left\{\frac{1}{h}\left(\frac{\partial^2 v_\xi}{\partial \xi^2} + \frac{\partial^2 v_\xi}{\partial \eta^2}\right)\right. \qquad (14)$$
$$-\frac{2}{a}\left(\sinh\eta\frac{\partial v_\eta}{\partial \xi} - \sin\xi\frac{\partial v_\eta}{\partial \eta}\right)$$
$$\left.-\left(\frac{\cosh\eta + \cos\xi}{a}\right)v_\xi\right\},$$

$$\frac{\partial v_\eta}{\partial t} + \frac{1}{h}\left(v_\xi \frac{\partial v_\eta}{\partial \xi} + v_\eta \frac{\partial v_\eta}{\partial \eta}\right) + v_z \frac{\partial v_\eta}{\partial z}$$
$$+\frac{1}{a}\left(\sinh\eta (v_\xi)^2 - \sin\xi (v_\xi v_\eta)\right) = -\frac{1}{h}\frac{1}{\rho}\frac{\partial p}{\partial \eta}$$
$$+\nu\frac{\partial^2 v_\eta}{\partial z^2} + \frac{\nu}{h}\left\{\frac{1}{h}\left(\frac{\partial^2 v_\eta}{\partial \xi^2} + \frac{\partial^2 v_\eta}{\partial \eta^2}\right)\right.$$
$$\left.+\frac{2}{a}\left(\sinh\eta\frac{\partial v_\xi}{\partial \xi} - \sin\xi\frac{\partial v_\xi}{\partial \eta}\right) - \left(\frac{\cosh\eta + \cos\xi}{a}\right)v_\eta\right\}, \qquad (15)$$

$$\frac{\partial v_z}{\partial t} + \frac{1}{h}\left(v_\xi \frac{\partial v_z}{\partial \xi} + v_\eta \frac{\partial v_z}{\partial \eta}\right) + v_z \frac{\partial v_z}{\partial z} = \qquad (16)$$

$$-\frac{1}{\rho}\frac{\partial p}{\partial z} + \nu\left\{\frac{1}{h^2}\left(\frac{\partial^2 v_z}{\partial \xi^2} + \frac{\partial^2 v_z}{\partial \eta^2}\right) + \frac{\partial^2 v_\xi}{\partial z^2}\right\},$$

$$\frac{1}{h^2}\left[\frac{\partial (h v_\xi)}{\partial \xi} + \frac{\partial (h v_\eta)}{\partial \eta}\right] + \frac{\partial v_z}{\partial z} = 0, \qquad (17)$$

where v_ξ, v_η and v_z are the physical components of velocity vector $v = (v_\xi, v_\eta, v_z)$, p is the pressure, $\nu = \frac{\mu}{\rho}$ is the coefficient of kinematic viscosity and $h = \frac{a}{(\cosh\eta - \cos\xi)}$.

In the present situation the boundary conditions are a no-slip requirement on cylinders

$$v_\xi = \omega_i r_i,\ v_\eta = 0, \text{ on } \eta = \eta_i, \xi \in [0, 2\pi), i = 1, 2, \qquad (18)$$

where $\omega_i, i = 1, 2$ are rotational velocities of the cylinder walls. Positive values of $\omega_i, i = 1, 2$ correspond to counterclockwise rotation. Upstream and downstream boundary conditions at infinity are

$$v_x = 0,\ v_y = U_\infty, \quad as\ r^2 = x^2 + y^2 \to \infty, \qquad (19)$$

where v_x and v_y are components of the velocity vector in x and y directions respectively. Self motion requires that the resultant fluid force and torque on the combined system of the two cylinders are zero. The net force exerted by fluid on an immersed body with surface $\sum$ is

$$F = \int_\sum \tau\, dS, \quad M = \int_\sum [r \times \tau]\, dS,$$

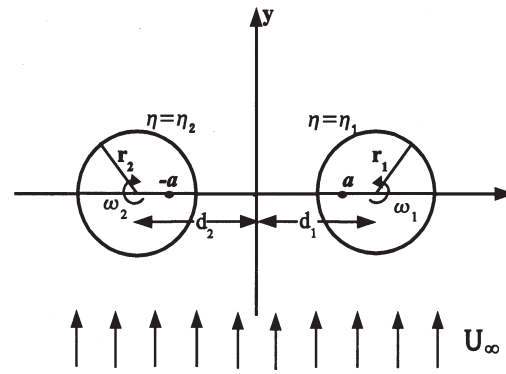

Figure 1. Geometrical sketch of the flow scheme

where $\tau = T(v,p)\cdot n$ is the stress vector. The force per unit area exerted across a rigid boundary element with outward normal n in an incompressible fluid is defined by

$$\tau = -pn - \mu(n\times\omega)$$

where p is pressure and ω is vorticity defined as $\omega = \operatorname{curl} v$. If F_{x_i} and $F_{y_i}, i = 1, 2,$ are the lift and drag on the cylinders, the lift and drag coefficients are defined by

$$C_{L_i} = \frac{F_{x_i}}{\rho U_\infty D}, \quad C_{D_i} = \frac{F_{y_i}}{\rho U_\infty D}, \quad i = 1, 2,$$

And each consists of components due to the friction forces and the pressure. Hence

$$C_L = C_{L_f} + C_{L_p}, \quad C_D = C_{D_f} + C_{D_p},$$

Where

$$C_{L_f} = -\frac{1}{\rho U_\infty D}\int_\Sigma \mu(n\times\omega)\cdot i_x \, dS,$$

$$C_{D_f} = -\frac{1}{\rho U_\infty D}\int_\Sigma \mu(n\times\omega)\cdot i_y \, dS,$$

$$C_{L_p} = -\frac{1}{\rho U_\infty D}\int_\Sigma pn\cdot i_x \, dS,$$

$$C_{D_p} = -\frac{1}{\rho U_\infty D}\int_\Sigma pn\cdot i_y \, dS.$$

Here i_x, i_y are unit vectors in x and y axes directions.

The problem of self-motion is to find solution of the Navier-Stokes Eqns. (14) - (17) with boundary conditions (18) - (19) and additional constraints

$$F = M = 0 \tag{20}$$

Eqn. (20) establishes the basic distinction between stationary flow over self-propelled and towed bodies. The numerical simulation of the flow past self-moving bodies becomes more complicated as a result of the nonlocality of constraints like (20). For such flows, the results depend not only on the Reynolds number Re but also on the non-dimensional gap spacing between the two cylinders, g, and on parameters, α_i representing the ratios of the rotational velocities of the cylinder walls to the oncoming flow velocity

$$\mathrm{Re} = U_\infty D/v, \quad \alpha_i = D\omega_i/2U_\infty, \quad i = 1, 2,$$

and $g = \dfrac{d - r_1 - r_2}{D}$,

where ω_i are constant angular velocities of the cylinders' rotation, U_∞ is the oncoming free stream velocity and v is the kinematic viscosity of the fluid.

Numerical Algorithm

The algorithm of the problem solution is based on the concept of projection methods (Chorin, 1968). Let us only recall that intermediate velocity components $\tilde{v}_\xi, \tilde{v}_\eta$ are computed in a first step by solving a finite difference approximation of the momentum equations

$$\tilde{\vec{v}} = \vec{v}^n - \tau\left((\vec{v}^n\cdot\nabla)\vec{v}^n - \frac{1}{\mathrm{Re}}\Delta\vec{v}^n\right) \tag{21}$$

$$-\nabla(\kappa\, p^n); \quad \kappa = 0 \text{ or } 1$$

and intermediate velocity vector (which is not solenoidal) is then decomposed into divergence free and rotational free vector fields by solving the Poisson equation with homogeneous Neumann boundary conditions

$$\tilde{\vec{v}} = \vec{v}^{n+1} + \tau\nabla\Phi, \quad \operatorname{div}\vec{v}^{n+1} = 0. \tag{22}$$

$$\begin{cases} \Delta\Phi = \dfrac{1}{\tau}\operatorname{div}\tilde{\vec{v}}, \\ \dfrac{\partial\Phi}{\partial n} = 0. \end{cases} \tag{23}$$

The final approximation of the $\vec{v}$ and p at time $t^{n+1} = (n+1)\Delta t$ can be found as follows:

$$\vec{v}^{n+1} = \tilde{\vec{v}} - \tau\nabla\Phi, \quad \Phi + \kappa\, p^n = p^{n+1} \text{ or}$$

$$\Phi + \kappa\, p^n = \frac{p^n + p^{n+1}}{2}.$$

The staggered arrangement of the different variables is used. The velocity components are located at the center of the cell edges and are normal to them. Scalar functions such as pressure and divergence are located at the cell centers. For the purpose of determining an

intermediate velocity an explicit approximation of Eqn. (21) is employed. The scheme of stabilizing correction (Yanenko, 1971), also called the second Douglas scheme (Douglas and Rachford, 1956), is utilized to find an approximate solution of (22). The steady-state computed solution is defined by

$$\frac{\left\|\theta^{n+1}-\theta^{n}\right\|}{\Delta t\left\|\theta^{n+1}\right\|}<\varepsilon, \qquad (24)$$

where $\theta=(v_\xi, v_\eta, C_D, C_L)$; Δt is the time step and θ^n refers to the numerical approximation at time $n\Delta t$, ε is sufficiently small positive number (ε have been chosen such that variation of C_D and C_L on the large time interval less than 0.1%). Figure 2 shows the grid construction and the location of unknown functions. The boundary conditions (19) corresponding to $r\to\infty, (\eta=0, \xi=0;\ \eta=0, \xi=2\pi)$ were translated to boundaries which are sufficiently far from the cylinders in physical space. These boundaries are shown in Figure 2 by bold solid lines. The inflow and outflow boundaries have a Dirichlet boundary condition $(v_x=0, v_y=1)$. The no-slip condition is imposed on the cylinders' surface and the periodic boundary condition $\Psi(0,\eta)=\Psi(2\pi,\eta)$ is used on the boundaries $\xi=0$ and $\xi=2\pi$ (here Ψ denotes one of the unknown functions v_ξ, v_η, p and Φ) All the numerical simulations are continued until the flow reaches a fully developed state, where all the flow characteristics are analyzed.

Validation of Numerical Algorithm

It is well known that for large gap spacing between the two surfaces of the cylinders the mutual influence between cylinders disappears, leading to separate flow over single cylinders. To validate the present numerical algorithm, the uniform flow past fixed and rotating circular cylinders with $0\le \mathrm{Re}\le 40, 0\le \alpha_1 (=\alpha_2)\le 2.5$ and with a large gap between cylinder surfaces $g=14$ have been calculated and the results

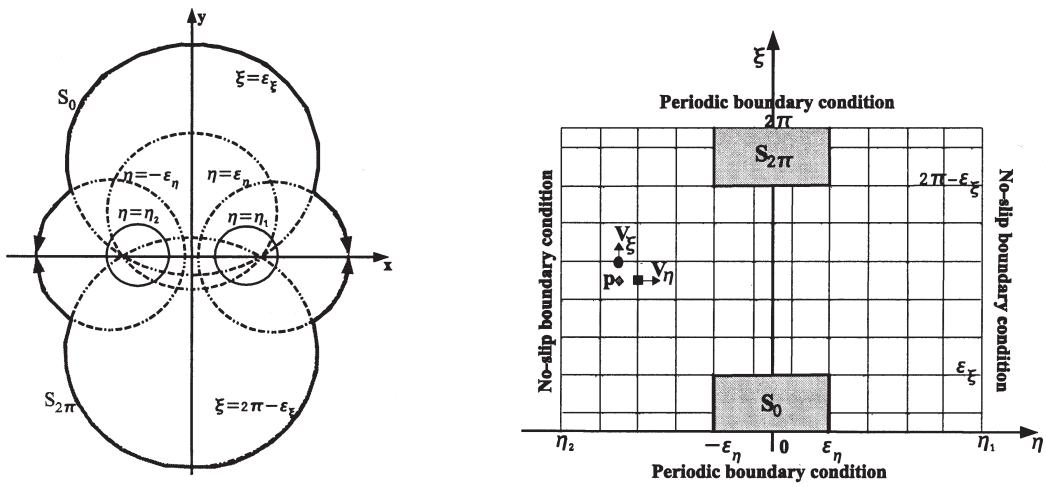

Figure 2. Transformation between physical domain and computational domain

compared with experimental and simulation data for flow past a single cylinder. All the simulations have been performed in a large domain so as to reduce the influence of the outer boundary. A sequence of uniform grids is used. Because the cylinder wake is stable to perturbations in the flow regime below $\mathrm{Re} \le 46 \pm 1$, the flow will reach a steady state for $\mathrm{Re} \le 40$. The calculated nondimensional steady-state wake length L_W (the distance from the cylinder trailing edge to the reattachment point) and the drag coefficient $C_D = C_{D_p} + C_{D_f}$ are compared with previously established results. The current results of wake length and drag coefficient are compared to the numerical simulations and experimental data in Table 1. In this table C_{D_p} and C_{D_f} denote the pressure and friction drag coefficients, respectively. The spatial resolution of the mesh is shown in curly brackets. The comparisons show that the present results are in good agreement with previous results.

To the authors' knowledge, there are very few published data of drag and lift coefficients at $\mathrm{Re} \le 40$ and angular speed even for flow past single cylinders. Table 2 lists the calculated lift and drag coefficients and makes a comparison with Badr *et al.* (1989), Ingham and Tang (1990) and Chung (2006). It can be seen that the differences are acceptable for C_D and C_L. For the case of a large gap between cylinders the streamline patterns are similar to those in the flow behind a single cylinder, (Batchelor, 2000 and Chung, 2006). The steady-state streamline patterns in Figure 3 (a) shows the recirculation region behind the cylinder (left) at $\mathrm{Re} = 20, \alpha = 0, g = 14$. For $\mathrm{Re} = 20$, the flow induced by several angular speeds in interval $0 \le \alpha_i \le 2.5$ have been computed. Figures 3(b) and 3(c) show the

Table 1. Validation of the numerical algorithm; comparison study for flow over two side-by-side circular cylinders at g = 14 with flow over a single cylinder

Re	Contribution	C_D	C_{D_p}	C_{D_f}	L_w/D
5	Present (20×20)	3.748	1.883	1.865	
	Present (40×40)	4.050	2.099	1.960	
	Ingham and Tang (1990) (one cylinder)	3.997	2.104	1.843	
	Batchelor (2000) (one cylinder)	3.995	---	---	
20	Present (20×20)	2.022	1.193	0.829	
	Present (40×40)	2.069	1.229	0.840	
	Present (80×80)	2.120	1.270	0.850	0.890
	Relf (1913) (one cylinder)	2.160	---	---	
	Tritton (1959) (one cylinder)	2.080	---	---	
	Chung (2006) (one cylinder)	2.050	---	---	0.960
	Ingham and Tang (1990) (one cylinder)	1.995	1.201	0.794	
	Batchelor (2000) (one cylinder)	2.001	---	---	0.900
40	Present (40×40)	1.539	1.002	0.537	2.160
	Relf (1913) (one cylinder)	1.620	---	---	
	Tritton (1959) (one cylinder)	1.590	---	---	
	Chung (2006) (one cylinder)	1.540	---	---	2.300
	Batchelor (2000) (one cylinder)	1.538	---	---	2.150

predicted steady-state streamline patterns for $\alpha = 0.1$ and $\alpha = 1.0$, respectively. Due to symmetry we only represent the streamline patterns around one cylinder (left) in Figure 3.

The accuracy and grid independence of the numerical results is checked by computations on various grids. The simulation was carried out on three grids with $h_{\xi 1} = 0.16535$, $h_{\eta 1} = 0.17436$, $h_{\xi 2} = 0.080554$, $h_{\eta 2} = 0.086078$, $h_{\xi 3} = 0.039767$, $h_{\eta 3} = 0.042759$. The time step size $\Delta t = 0.001$. Some data on comparisons of the calculation results are represented in Table 3.

In the case of $\mathrm{Re} = 40$ and g = 1 the computed drag coefficients for both cylinders are nearly the same and the lift coefficients are in the opposite directions. There is about 5 ~ 7% difference in C_D between the present calculations and the result reported by Kang (2003) at $\mathrm{Re} = 40$, g = 1. Figure 4 shows steady-state streamline patterns behind the cylinders at $\mathrm{Re} = 40$, α = 0 and g = 1. Wake patterns are similar to those in Kang (2003). The comparisons made in Tables 1 and 2 and in Figures 3 and 4 indicate the appropriateness of the numerical method and mesh used in this study.

Results and Discussion

After verifying the numerical method, we have conducted numerical simulations of flow past constantly rotating circular cylinders of equal radii in a side-by-side arrangement at Reynolds numbers Re = 10, 20 and 40, rate of rotation $0.5 \le \alpha \le 2.5$ and nondimensional gap spacing

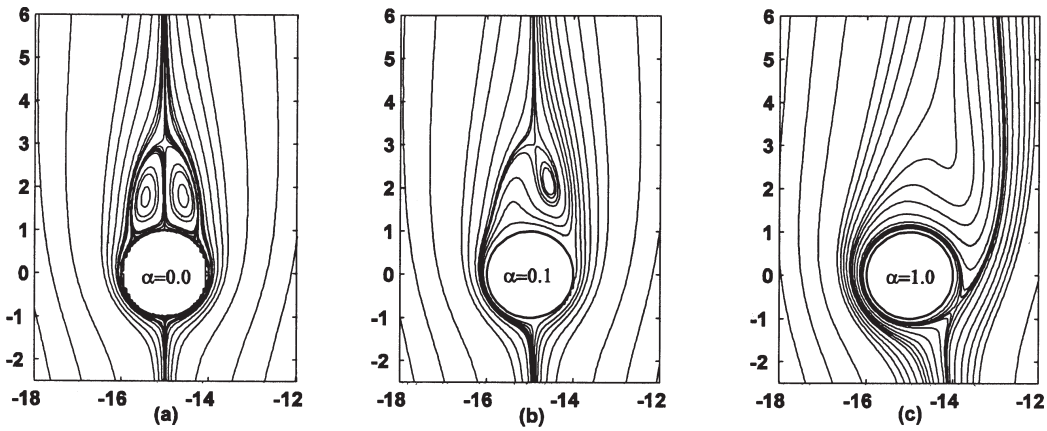

Figure 3. Streamline patterns of flow over two circular cylinders at Re = 20, g = 14 and α = 0.0, 0.1, 1.0

Table 2. Hydrodynamic parameters of flow over a rotating circular cylinder at Re = 20 with g = 14

Re	Contribution	C_D			C_L		
		$\alpha = 0.1$	$\alpha = 1.0$	$\alpha = 2.0$	$\alpha = 0.1$	$\alpha = 1.0$	$\alpha = 2.0$
20	Present (80×80)	2.119	1.887	1.363	0.291	2.797	5.866
	Badr *et al*. (1989)	1.990	2.000	---	0.276	2.740	---
	Ingham and Tang (1990)	1.995	1.925	1.627	0.254	2.617	5.719
	Chung (2006)	2.043	1.888	1.361	0.258	2.629	5.507

$g = 1$. Both cylinders are placed in a stream (from down to up) of uniform speed U_∞ at infinity. The left cylinder is rotating with constant clockwise angular velocity. The right cylinder is rotating with the same constant anti-clockwise angular velocity. The sketch of the present problem is shown in Figure 1.

The influence of the rotation rate $\alpha = \alpha_1 = \alpha_2 = |\omega_i| D/2U_\infty$ is demonstrated in Table 4 and Figure 5. Table 4 gives the values of drag and lift coefficients in cases Re = 10, 20 and $g = 1$ for $0.5 \le \alpha \le 2.5$ Indexes 1 and 2 correspond to the right and left cylinders, respectively. The fluid forces are distributed over the two cylinders such that lift forces in x-direction on the combined system are in equilibrium, $C_{L_1} + C_{L_2} \equiv 0$. However, the fluid forces acting upon an individual cylinder demand that some additional external forces are applied to it in order for its position to remain fixed. There is a repulsive force acting on the cylinders, $C_{L_1} > 0, C_{L_2} > 0$. The absolute values of lift coefficients increase with increasing α, as shown in the sixth column of Table 4. The lift forces acting on cylinders mostly result from the pressure force, as can be seen in the two last columns of Table 4. The pressure contribution in C_L increases with increasing Re, which is the same behavior as observed in the study of Stojkovic *et al.* (2002) for the case of a single rotating cylinder. The drag coefficients decrease with increasing α, (see third column of Table 4). For $\alpha \approx 1.65$ (Re = 10) and $\alpha \approx 1.74$ (Re = 20) the drag force becomes zero.

Table 3. Sequence of grid; drag and lift coefficient at Re = 20, g = 14 and α = 0.1

grid	C_D	C_{D_p}	C_{D_f}	C_L	C_{L_p}	C_{L_f}
(40×40)	1.858	1.033	0.825	2.740	2.393	0.347
(80×80)	1.887	1.061	0.826	2.797	2.437	0.360
(160×160)	1.901	1.074	0.827	2.802	2.440	0.362

Table 4. Drag and lift coefficient of flow over two rotating circular cylinders at Re = 10 and 20 with g = 1

α	Re	C_D	C_{D_p}	C_{D_f}	$C_{L_{1,2}}$	$C_{L_{p1,2}}$	$C_{L_{f1,2}}$
0.5	10	1.942	1.219	0.723	±2.181	±1.623	±0.558
	20	1.485	0.919	0.566	±1.721	±1.382	±0.339
1.0	10	1.094	0.824	0.270	±3.028	±2.355	±0.673
	20	0.862	0.530	0.332	±2.774	±2.300	±0.474
1.5	10	0.247	0.440	-0.193	±3.544	±2.811	±0.733
	20	0.260	0.151	0.109	±3.645	±3.065	±0.580
1.65	10	0.004	0.335	-0.331	±3.633	±2.894	±0.739
1.74	20	-0.001	-0.004	0.003	±3.958	±3.345	±0.613
2.0	10	-0.516	0.134	-0.650	±3.713	±2.983	±0.730
	20	-0.265	-0.152	-0.113	±4.196	±3.563	±0.633
2.5	10	-1.199	-0.076	-1.123	±3.415	±2.767	±0.648
	20	-0.685	-0.330	-0.355	±4.214	±3.608	±0.606

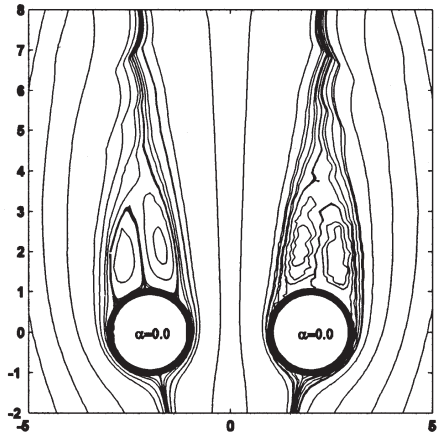

Figure 4. Streamline patterns of flow over two circular cylinders at Re = 40, g = 1 and α = 0.0

This case corresponds to the self-propelled motion of cylinders as a coupled body. It is interesting that both C_{D_p} and C_{D_f} decrease with increasing α, (see columns 4 and 5 in Table 4), resulting in negative values of C_{D_p} and C_{D_f} for higher rotational velocities. This is opposite to the case of flow past a single rotating cylinder, where C_{D_f} increases and C_{D_p} decreases with increasing α (Stojkovic *et al.,* 2002). Additionally, for $\alpha \geq 2.0$ the total drag force is negative because C_{D_f} dominates over C_{D_p}. In the case of flow around a single rotating cylinder the effect is quite different. It has to be pointed out that the self-propelled regime happened due to different reasons at Re = 10 and at Re = 20. In the case of Re = 10 the drag $C_D \approx 0$ is due to

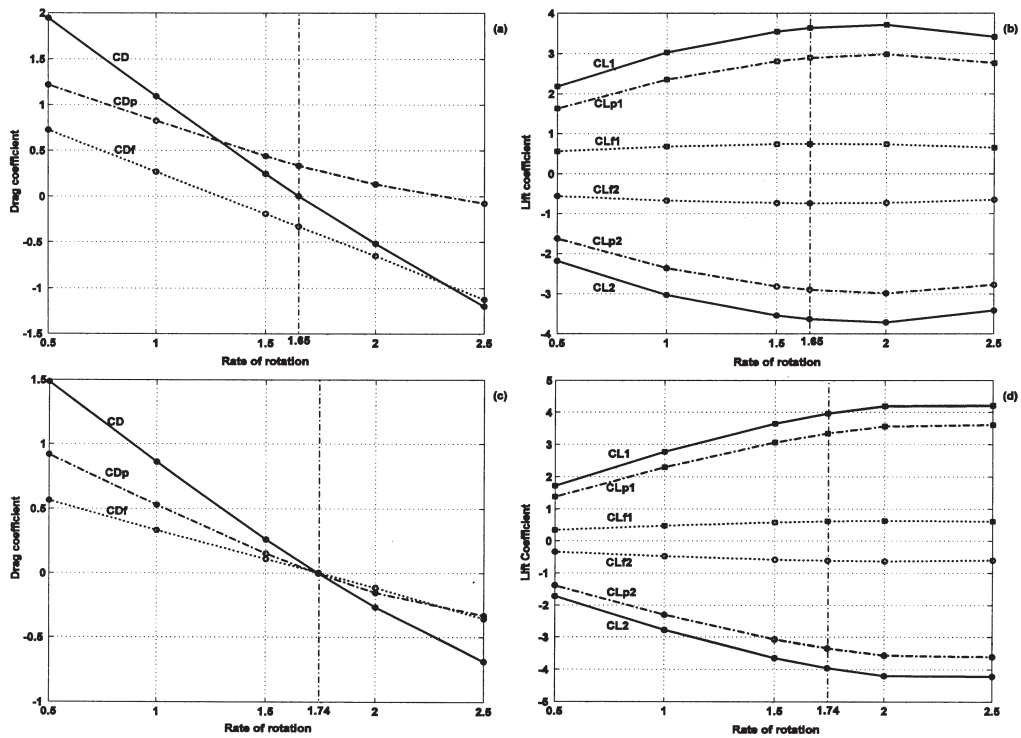

Figure 5. Drag and lift coefficients at Re = 10(*a*) - (*b*), 20(*c*) - (*d*) and g = 1, $\alpha \in [0.5, 2.5]$

$C_{D_p} \approx -C_{D_f} \approx 0.33$. In the case of Re = 20 the self-propelled regime corresponds to $C_D \approx 0$ due to $C_{D_p} \approx -C_{D_f} \approx 0$. Figure 5 demonstrates the dependence of lift and drag coefficient on rate of rotation. Figures 5(a) - 5(b) correspond to Re = 10 and g = 1. Figures 5(c) - 5(d) correspond to Re = 20 and g = 1. At Re = 10 drag coefficient decreases almost linearly with increasing α. Both coefficients C_{D_p} and C_{D_f} also decrease linearly with increasing α and it is easy to see that C_{D_f} decreases faster than C_{D_p}. At Re = 20, C_{D_p} decreases faster than C_{D_f} up to $\alpha = \alpha$.

Figures 6 and 7 show the streamline patterns corresponding to the case Re = 10(20), g = 1.0 and α = 0.5, 1.0(1.5), 1.65*(1.74*), 2.0. All are symmetrical about the y - axis. There are regions of closed streamlines near the cylinders for all values of α. These streamlines only exist very close to the cylinders for small values of α. However, as α increases they exist in larger and larger regions as illustrated in Figures 6 and 7. For small α the space between regions of closed streamlines is sufficiently large that fluid can go through the gap between the cylinders, (Figures 6(a) and 7(a)). As α increases the stagnation points rotate in the direction opposite to the direction of the cylinders' rotation and depart from the surfaces of the cylinders and approach the y - axis at the smallest spacing between the cylinders. Finally, the space between the cylinders' surfaces becomes narrower further increasing the closed streamlines' regions. At α between ~1.0 and ~1.5 these regions touch each other along the y - axis. The stagnation points are now located on the y - axis, both upstream and downstream, as illustrated in Figures 6(b) - 6(d) and 7(b) - 7(d). Further increases in angular velocity of the cylinders is a reason of increasing of closed contour regions around the cylinders, (Figures 6(c) - 6(d) and 7(c) - 7(d)). The stagnation points on the y - axis move upstream and downstream of the cylinders. The downstream stagnation point moves far away from the line between the center of the cylinders. The streamline patterns of the self-propelled regime are represented by Figures 6(c) and 7(c) for Re = 10 and Re = 20, respectively.

Conclusion

In this paper, we have represented a numerical study of steady two-dimensional viscose fluid flow past the two circular cylinders of equal radii which rotate with opposite angular velocity. Validation of the numerical algorithm has been performed by comparison of the present results of uniform flow past two fixed and rotating circular cylinders with experimental and numerical data for flow past a single cylinder.

Simulations were performed for flows with $5 \le \mathrm{Re} \le 40$ in the range $0 \le \alpha \le 2.5$ and gap spacing, g = 1 The rotation of the circular cylinders in a viscous uniform flow significantly modified flow patterns and reduced drag and lift forces acting on each cylinder compared with the case of uniform flow over cylinders with $\alpha = 0$.

Results showed that two separate regions of closed streamlines near cylinders exist at low rotation speed. A further increase in angular velocity of the cylinders generates the region of fluid which encloses both the right and left cylinders. This region consists of two subregions of closed streamlines which connected along the y - axis. Two stagnation points exist on the y - axis. The drag coefficient vanishes at $\alpha = \alpha^*$. The critical rotation speed α^* depends on the Reynolds number, for example $\alpha^* \approx 1.65$ and 1.74 for Re = 10 and 20, respectively. The value of α^* corresponds to the self-propelled motion of two cylinders as a coupled body. The lift force acting on each cylinder increases with increasing α. The lift force mostly results from the pressure contribution. The drag force decreases

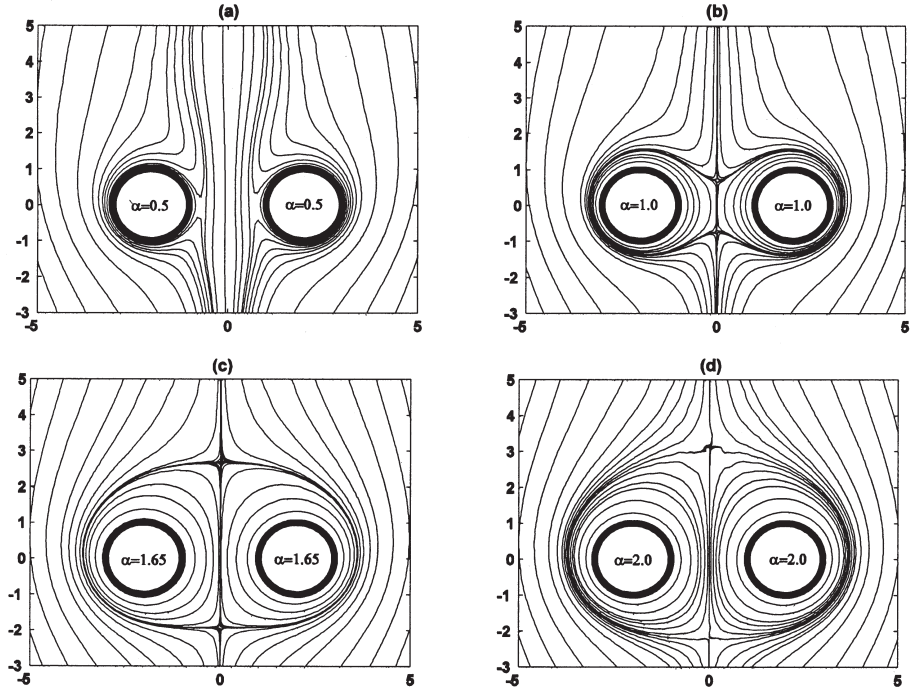

Figure 6. Streamline patterns of flow over two circular cylinders at Re = 10, g = 1 and α = 0.5, 1.0, 1.65, 2.0

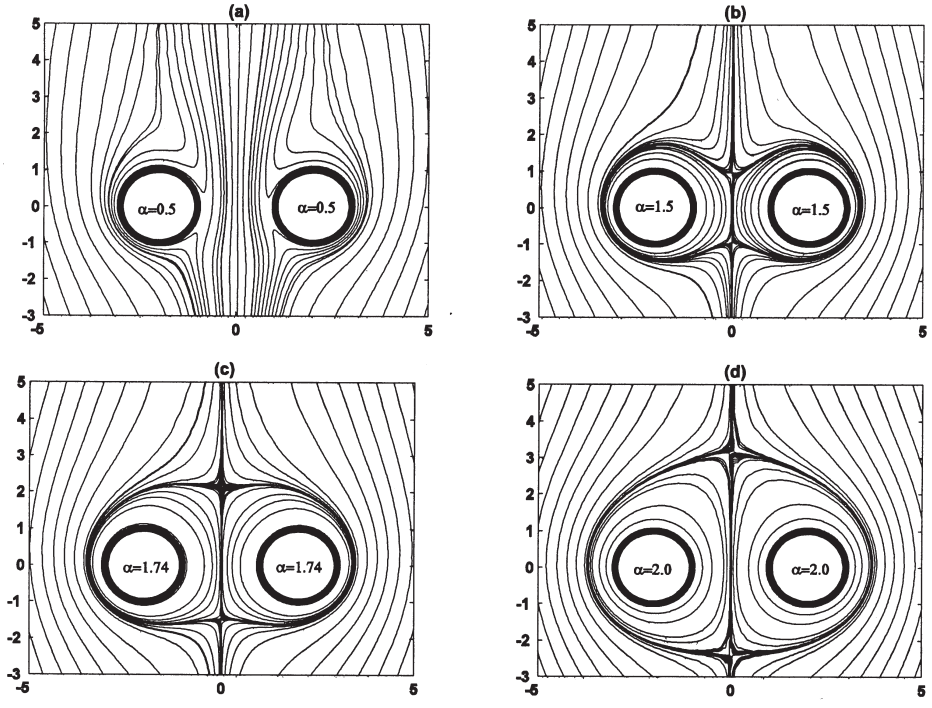

Figure 7. Streamline patterns of flow over two circular cylinders at Re = 20, g = 1 and α = 0.5, 1.5, 1.74, 2.0

with increasing α, in particular both C_{D_p} and C_{D_f} decrease with increasing α.

References

Badr, T., Dennis, S.C.R., and Young, P.J.S. (1989). Steady and unsteady flow past a rotating circular cylinder at low Reynolds numbers. Computers & Fluids, 17(4):579-609.

Batchelor, G.K. (2000). Introduction to Fluid Dynamics. Cambridge University Press, Cambridge, UK, 615 p.

Chorin, A.J. (1968). Numerical solution of the Navier-Stokes equations. Math. Comp., 22:745-762.

Chung, M-H. (2006). Cartesian cut cell approach for simulating incompressible flows with rigid bodies of arbitrary shape. Computers & Fluids, 35(6):607-623.

Danielson, D.A. (1997). Vectors and Tensors in Engineering and Physics. 2nd ed. Perseus Books, Cambridge, MA, USA, 282 p.

Douglas, J., and Rachford, H.H. (1956). On the numerical solution of heat conduction problem in two and three space variables. Trans. Amer. Math. Soc., 82:421-439.

Elliot, L., Ingham, D.B., and Bashir, T.B.A.El. (1995). Stokes flow past two circular cylinders using a boundary element method. Computers & Fluids, 24(7): 787-798.

Finn, R. (1965). On the exterior stationary problem for the Navier-Stokes equations and associated perturbation problems. Arch. Rational Mech. Anal., 19:363-406.

Galdi, G.P. (1997). On the steady, translational self-propelled motion of a symmetric body in a Navier- Stokes fluid. Quad. Mat. II Univ. Napoli, 1:97-169.

Galdi, G.P. (1999). On the steady self-propelled motion of a body in a viscous incompressible fluid. Arch. Rational Mech. Anal., 148: 53-88.

Ingham, D.B., and Tang, T. (1990). A numerical investigation into the steady flow past a rotating circular cylinder at low and intermediate Reynolds numbers. J. Comput. Phys., 87:91-107.

Izteleulov, M.I. (1985). Calculation of momentumless flow past an ellipsoid. Problemy Dinamiki Vyazkoi Zidkosti, Novosibirsk, Russia, p. 21-32.

Jeffery, G.B. (1922). The rotation of two circular cylinders in a viscous fluid. Proceedings of the Royal Society of London. Series A; May 1, 1922; London, UK, Containing Papers of a Mathematical and Physical Character, 101(709):169-174.

Kang, S. (2003). Characteristics of flow over two circular cylinders in a side-by-side arrangement at low Reynolds numbers. Phys. of Fluids, 15(9):2,486-2,498.

Khonichev, V.I., and Yakovlev, V.I. (1978). Motion of a sphere in an infinite conductive fluid, produced by a variable magnetic dipole located within the sphere. J. Appl. Mech. Tech. Phys., 19(6):760-765.

Lugovtsov, A.A., and Lugovtsov, B.A. (1971). The example of viscous incompressible flow past a body with a moving boundary. Dinamika Sploshnoi Sredy, Novosibirsk, Russia, p. 8.

Milne-Thomson, L.M. (1952). Theoretical Aerodynamics. Van Nostrandt Co., NY, USA.

Moshkin, N.P. (1991). On certain examples of numerical modeling of a steady flow past a self-propelled sphere. Russian Journal of Theoretical and Applied Mechanics, 1(2):111-125.

Moshkin, N.P., Pukhnachev V.V., and Sennitskii, V.L. (1989). Numerical and analytical investigations of a stationary flow past a self-propelled body. Proceedings of Fifth International Conference on Numerical Ship Hydrodynamics, Part 1; 25-28 September 1989; Hiroshima, Japan, p. 238-248.

Nakanishi, M., and Kida, T. (1999). Unsteady low Reynolds number flow past two rotating circular cylinders by a vortex method. Proceedings of the 3rd ASME/JSME Joint Fluid Engineering Conference; July 18-23, 1999; San Frantsisco, California, USA.

Pukhnachev, V.V. (1989). Asymptotics of a velocity field at considerable distances

from a self-propelled body. J. Appl. Mech. Tech. Phys., 30:52-60.

Pukhnachev, V.V. (1990). The problem of momentumless flow for the Navier-Stokes Equations. In: Lecture Notes in Mathematics, 1431, Springer-Verlag, NY, p. 87-94.

Relf, E.F. (1913). Discussion of the results and measurements of the resistance of wires, with some additional tests on the resistance of wires of smaller diameter. Tech Rep and Memo. Adv Comm Aero(ACA), London, Uk, 102 p.

Sennitskii, V.L. (1973). Viscous incompressible fluid flow past rotating cylinders. Dinamika Sploshnoi Sredy, Novosibirsk, Russia, 14:71-88.

Sennitskii, V.L. (1975a). Rotating cylinders in a viscous liquid. Part 1. Dinamika Sploshnoi Sredy, Novosibirsk, Russia, 21:70-83.

Sennitskii, V.L. (1975b). Rotating cylinders in a viscous liquid. Part 2. Dinamika Sploshnoi Sredy, Novosibirsk, Russia, 23:169-181.

Sennitskii, V.L. (1978). Liquid flow around a self-propelled body. J. Appl. Mech. Tech. Phys., 3:15-27.

Sennitskii, V.L. (1980). On the propelling of a pair of rotating circular cylinders in a liquid. Dinamika Sploshnoi Sredy, Novosibirsk, Russia, 47:145-153.

Sennitskii, V.L. (1981). On the drag force acting on a pair of circular cylinders streamed by water. Dinamika Sploshnoi Sredy, Novosibirsk, Russia, 52:178-182.

Sennitskii, V.L. (1984). An example of axisymmetric fluid flow around a self-propelled body. J. Appl. Mech. Tech. Phys., 4:31-36.

Sennitskii, V.L. (1990). Self-propulsion of a body in a fluid. J. Appl. Mech. Tech. Phys., 31:266- 272.

Shatrov, V.I and Yakovlev, V.I. (1985). Hydro-dynamic drag of a ball containing a conduction-type source of electromagnetic fields. J. Appl. Mech. Tech. Phys., 26:19-24.

Silvestre, A.L. (2002a). On the self-propelled motion of a rigid body in a viscous liquid and on the attainability of steady symmetric self-propelled motions. J. Math. Fluid Mech., 4:285-326.

Silvestre, A.L. (2002b). On the slow motion of a self-propelled rigid body in a viscous incompressible fluid. J. Math. Anal. Appl., 274:203-227.

Smith, S.H. (1991). The rotation of two circular cylinders in a viscous fluid. Mathematika, 38(63).

Stojkovic, D., Breuer, M., and Durst, F. (2002). Effect of high rotation rates on the laminar flow around a circular cylinder. Phys. of Fluids, 4(9):3,160-3,178.

Tritton, D.J. (1959). Experiments on the flow past a circular cylinder at low Reynolds number. J. Fluid Mech., 6:547.

Watson, E.J. (1995). The rotation of two circular cylinders in a viscous fluid, Mathematika, 42(1):105.

Yanenko, N.N. (1971). Method of Fractional Steps, 1st ed. Gordan and Breach, NY, USA, 160 p.